Mon. Not. R. astr. Soc. (1968) **140**, 197–221.

THE ABUNDANCES OF THE ELEMENTS IN THE SOLAR PHOTOSPHERE—V

The Alkaline Earths Mg, Ca, Sr, Ba

D. L. Lambert and B. Warner

(Received 1967 December 18)

Summary

A detailed account is given of available solar absorption lines arising from the neutral and ionized alkaline earth elements. Careful use of theoretical and experimental oscillator strengths leads to the following revized abundances, on the scale where $\log N(\mathrm{H}) = 12{\cdot}00$:

$$\log N(\mathrm{Mg}) = 7{\cdot}48$$
$$\log N(\mathrm{Ca}) = 6{\cdot}33$$
$$\log N(\mathrm{Sr}) = 2{\cdot}82$$
$$\log N(\mathrm{Ba}) = 1{\cdot}90$$

1. *Introduction*

Although abundance estimates for the alkaline earth elements—Mg, Ca, Sr, Ba—are available (see for example Goldberg, Müller & Aller (1960); subsequently referred to as GMA), this new study of the appearance of the alkaline earths in the Fraunhofer spectrum incorporates several novel features which permit their abundances to be re-evaluated with greater accuracy.

The magnesium abundance quoted by GMA was based on a study of eleven Mg I lines. The Mg I spectrum is restudied in this paper but the abundance analysis is restricted to a carefully selected group of lines. The selection criteria are discussed fully in Section 2.1.3. Only two of the eleven lines listed by GMA satisfy the present criteria. The principal novel feature of this discussion of the magnesium abundance is the presentation of the first detailed analysis of the Mg II lines which are present in the Fraunhofer spectrum. The independent estimates for the magnesium abundance obtained from the first and second spectra are in reasonable agreement. This result lends confidence in the final averaged abundance.

Magnesium and silicon are the dominant contributors of free electrons in the outer layers of the photosphere. An accurate abundance for these elements is, therefore, required for the computation of the gas and electron pressures. Calcium is a minor source of free electrons owing to its lower abundance. At the lower temperatures prevailing in stars of later spectral type than the Sun, magnesium and silicon will be predominantly neutral and calcium (with sodium and aluminium) will become a dominant contributor.

The calcium abundance has been the subject of several investigations (see for example GMA (1960); Müller & Mutschlecner (1964)). A noteworthy feature concerning the analysis of the Ca I spectrum is the existence of two series of accurate *relative* oscillator strengths measurements which include many lines which are conveniently observable in the Fraunhofer spectrum. In Section 3.1.2 a new

method is described for the conversion of these relative measurements to absolute scale. This paper includes in Section 3.3.3 the first attempt to derive the calcium abundance from the lines of the Ca II spectrum. Independent estimates from the Ca I and Ca II analyses are in excellent accord.

The discussions of the Sr (from Sr I and Sr II lines) and Ba (from Ba II lines) abundances are less extensive. This opportunity is taken to rediscuss their abundances following improvements in the experimental and theoretical oscillator strengths for the pertinent transitions.

The methods of abundance analysis which were outlined in the first paper of this series (Lambert 1968) were employed for the present analyses. The model solar atmosphere given in Paper I and subsequently modified by Lambert & Warner (1968b, Paper III) was adopted. The primary sources of equivalent widths were summarized in Paper II of this series (Section 1.2, Lambert & Warner 1968a). Detailed references are given to additional sources of equivalent widths quoted in this paper.

Throughout the paper, abundances will be frequently referred to the GMA values and only the logarithmic difference

$$[X] = \log N(X) - \log N(X)_{\mathrm{GMA}}$$

will be quoted. For reference purposes, the GMA abundances for these four elements were

$$\log N(\mathrm{Mg}) = 7{\cdot}40 \qquad \log N(\mathrm{Ca}) = 6{\cdot}15$$
$$\log N(\mathrm{Sr}) = 2{\cdot}60 \qquad \log N(\mathrm{Ba}) = 2{\cdot}10$$

on the normal scale where $\log N(\mathrm{H}) = 12{\cdot}00$.

2. *Magnesium*

2.1 *The Mg* I *spectrum*

2.1.1 *Introduction.* The occurrence of Mg I lines in the solar spectrum was reviewed recently by Swensson & Risberg (1966). These authors report that 219 Fraunhofer lines covering the wavelength interval 1800–24 566 Å can be attributed with certainty to Mg I. Their total includes 91 new identifications but, also, includes blended lines which are unsuitable for an abundance analysis. Nonetheless, it was apparent that the number of Fraunhofer lines attributed to Mg I and for which an accurate measurement of their equivalent width might be made exceeds 100. Owing to difficulties concerned with a lack of detailed knowledge of the continuous absorption coefficient, no lines with $\lambda < 4000$ Å are considered. Furthermore, in the absence of either extensive experimental measurements or a completely successful theoretical treatment of the oscillator strengths, the abundance analysis was based on a small and selected group of Mg I lines.

It is apparent by inspection of the term analysis of Mg I that the assumption of LS coupling is not widely applicable. For this reason, Warner (1968c) undertook intermediate coupling calculations. A detailed comparison of the results of these calculations with the solar equivalent widths is given in Section 2.1.4. It is apparent from that comparison that the intermediate coupling calculations provide more reliable oscillator strengths for certain transitions for which LS coupling is a poor approximation but an equally satisfactory treatment for all such transitions was not realized. The corollary of this statement was incorporated into the criteria governing the selection of Mg I lines for the abundance analysis: the Mg I transition

is included if the intermediate and LS coupling line strengths differ by less than about 5 per cent. This and additional selection criteria are described in the following section.

The lines rejected as unsuitable for the abundance analysis are further discussed in Section 2.1.4. The standard application of the curve of growth technique is reversed for these lines and the oscillator strength for the transition is derived from the solar equivalent width. Such values, which will be described as astrophysical oscillator strengths, may be usefully compared with the predictions of improved theoretical calculations.

2.1.2 *Mg* I *oscillator strengths.* The oscillator strengths used in this study are those calculated by Warner (1968c) from intermediate coupling theory and with allowance for configuration interaction. In Mg I, configuration mixing is particularly prominent in the $3snd\ ^1D$ levels, all of which are strongly mixed together and with $3p^2\ ^1D$. Unfortunately, many of the Mg I lines of astrophysical interest are transitions starting or ending on these ^1D levels. In the study of these, only levels up to $n = 7$ were included, so the allowance for configuration interaction is only a preliminary attempt at improving on LS-coupling line strengths. Some f-values changed by factors of up to a thousand between inclusion and non-inclusion of configuration interaction. It is clear, therefore, that we cannot expect the f-values to be of high accuracy when $3snd\ ^1D$ levels are involved. The astrophysical f-values given in Section 2.1.4 will be of help in later attempts at improving on the treatment of the ^1D levels.

A restriction (see next section) is placed on the use of transitions to high terms because the presence of configuration mixing in these has not been fully investigated.

2.1.3 *The magnesium abundance.* The abundance analysis is based on the 15 Mg I lines in Table I, which were selected from a list of about 80 unblended Fraunhofer lines identified in the list given by Swensson & Risberg (1966) as resulting from Mg I. Three principal selection criteria were adopted. Firstly, the LS and intermediate coupling line strengths were required to differ by less than 0·02 dex. Secondly, the principal quantum number of the upper (n') and lower (n'') levels should not differ by more than 3, that is $n' \leq n'' + 3$.

The group of lines selected on these two criteria was sufficiently numerous that a selection according to intensity or equivalent width was made. Lambert & Warner (1968b) discuss the problems encountered in the interpretation of the line profiles of strong Si I lines. Similar difficulties will apply to strong Mg I lines and to avoid these in the abundance analysis, the third criterion was formulated: the strength of the Fraunhofer line should not exceed $\log W_\lambda/\lambda = -5{\cdot}00$.

Details are given in Table I for the 15 lines satisfying the above requirements. Curves of growth were computed for the individual multiplets with correct allowance for line broadening although the restriction on the equivalent width ensures that the results are almost independent of the assumed damping constant.

There is a wide spread in the solutions from individual lines (see Table I): the range $-0{\cdot}25 < [\mathrm{Mg}] < +0{\cdot}20$ is approximately uniformly represented. This variation must be contrasted with the significantly smaller variations obtained from lines of a similar strength in the Mg II and Ca II spectra (Sections 2.2.3 and 3.3.3, respectively). This contrast strongly suggests that the greater portion of the

TABLE I

The Mg I lines which satisfy the selection requirements described in the text

RMT No.	Multiplet	ΔJ	$\lambda_\odot$ (Å)	χ (eV)	log gf	W_λ (mÅ)	$\log \frac{W_\lambda}{\lambda}+7$	[Mg]	Remarks*
22	$4s^3S$–$5p^3P^0$	1–0	7659·91	5·11	−1·82	30	1·59	−0·25	29L, 31RRT
23	$4s^3S$–$6p^3P^0$	1–2	6318·708	5·11	−1·72	48	1·88	−0·04	48PPC, 37RRT (1)
		1–1	6319·242	5·11	−1·94	28	1·65	−0·11	28PPC, 18RRT (1)
24	$4s^3S$–$7p^3P^0$	1–1	5785·561	5·11	−2·32	12	1·32	−0·13	RRT
25	$4s^1S$–$5p^1P^0$	0–1	8923·570	5·39	−1·39	54	1·78	−0·13	58L (3)
36	$4p^3P^0$–$7s^3S$	2–1	9993·17	5·93	−1·46	40	1·60	+0·16	L
		1–1	9986·490	5·93	−1·68	28	1·45	+0·20	L
		0–1	9983·23	5·93	−2·16	8·6	0·93	+0·12	L
35	$4p^3P^0$–$5d^3D$	0–1	10953·36	5·93	−0·86	97	1·95	−0·02	L
	$4p^3P^0$–$6d^3D$	0–1	9429·79	5·93	−1·25	31	1·52	−0·15	L
	$4p^3P^0$–$7d^3D$	1–1, 2	8712·701	5·93	−1·06	59	1·83	−0·01	59L, 57RRT
		0–1	8710·21	5·93	−1·54	21	1·38	−0·01	RRT
	$3d^3D$–$5p^3P^0$	−2	15879·54	5·94	−1·20	104	1·82	−0·15	Mo
		−1	15886·27	5·94	−1·42	68	1·63	−0·15	Mo
	$3d^3D$–$6p^3P^0$	−1	11033·64	5·94	−2·14	10	0·96	+0·08	L

Notes:

* The W_λ's from various sources are listed:

L ≡ Delbouille & Roland (1963)
RRT ≡ Moore, Minnaert & Houtgast (1966)
PPC ≡ Preliminary Photometric Catalogue, Utrecht (1960)
Mo ≡ Mohler (1955).

(1) The W_λ given by RRT is substantially smaller. A re-measurement of the Utrecht Atlas (Minnaert, Mulders & Houtgast 1940) gave results in good agreement with the adopted values.

(2) A small correction is made to the observed W_λ to allow for a weak Al I line, which contributes to the feature.

scatter can be attributed to inadequacies in the theoretical oscillator strengths. It is disappointing that this conclusion is reached when the lines were carefully chosen following a comparison of the LS and intermediate coupling calculations.

The mean abundance with the rms uncertainty is

$$[\mathrm{Mg}] = -0{\cdot}04 \pm 0{\cdot}03.$$

GMA included 11 lines from the Mg I spectrum in their discussion of the magnesium abundance. The intercombination line λ 4571 was included and for this they adopted an experimental measurement of the oscillator strength but, unfortunately, the available results were not in very close agreement. For the other ten lines, GMA adopted theoretical oscillator strengths provided by the coulomb approximation method and LS line strengths. It is of interest to inspect their line list using the present selection criteria. If the intercombination line is excluded, five of the remaining ten lines fail to satisfy the first criteria which requires that the oscillator strengths calculated on the basis of intermediate and of LS coupling agree to within 5 per cent. Another three lines are considered too strong with the result that only two lines satisfy all three criteria. The close agreement of the present value of the abundance with the GMA value is, therefore, largely fortuitous.

2.1.4 *Astrophysical oscillator strengths.* A total of 64 lines, which are assigned the identification Mg I, are listed in Table II. These lines failed to satisfy one or more of the three principal criteria discussed in the preceding section.

The astrophysical oscillator strengths obtained from the curve of growth are placed on an absolute scale assuming an abundance [Mg] = +0·08 (see Section 2.2.3). Their accuracy is typically ±0·10 dex or better with larger uncertainties for the very strong or very weak lines. The astrophysical oscillator strengths appear under the log *gf* heading in the column labelled (c). The log *gf* values obtained using coulomb approximation radial integrals and the LS line strengths are given in column (a). Column (b) gives the results of the intermediate coupling calculations (Warner 1968c).

A possible source of a systematic error affecting the astrophysical oscillator strengths must be mentioned. In order to obtain a satisfactory interpretation of the strong Si I profiles discussed in Paper III, it was sufficient to increase the calculated damping constants by a factor of about 2, in order to bring the predicted and observed line profiles into approximate coincidence. Although it was not proven that this increase was both necessary and sufficient, it was pointed out that line profile studies of the Na I D lines and the λ 7774 triplet indicated very similar deficiencies in the calculated damping constants.

Throughout the present calculations, the damping constants were calculated from the standard expressions for the radiative, van der Waals and Stark components. The total sum of downward transition probabilities and the Stark parameters ($\Delta\nu/E^2$) for each level were calculated and given on the computer output during the intermediate coupling calculations. The mean square radii required in the computation of the van der Waals broadening were computed from the STFD wavefunctions. Full details of the line broadening parameters for Mg I transitions are to be given by Warner in a paper now in preparation.

The adoption of the standard damping constant formulae may result in an overestimate for the astrophysical oscillator strength of strong lines: $\log W_\lambda/\lambda + 7 \geq 2{\cdot}30$. However, it is probable that the equivalent widths for these lines may be

TABLE II

Mg I *lines in the solar spectrum: astrophysical oscillator strengths*

RMT No.	Multiplet	ΔJ	$\lambda_\odot$ (Å)	χ (eV)	W_λ (mÅ)	$\log \frac{W_\lambda}{\lambda}+7$	log gf★ (a)	(b)	(c)	Remarks
1	$3s^2\ ^1S$–$3p^3P^0$	0–1	4571·102	0·00	95					
	$3p^1P^0$–$4s^1S$	1–0	11828·20	4·34	730	2·79	−0·30	−0·34	−0·17	
8	$3p^1P^0$–$5s^1S$	1–0	5711·095	4·34	120	2·32	−1·57	−1·43	−1·68	
10	$3p^1P^0$–$6s^1S$	1–0	4730·038	4·34	65	2·14	−2·09	−2·04	−2·21	
13	$3p^1P^0$–$7s^1S$	1–0	4354·514	4·34	34:	1·89	−2·43	−2·40	−2·63	
	$3p^1P^0$–$8s^1S$	1–0	4165·117	4·34	29:	1·84	−2·70	−2·67	−2·73	
	$3p^1P^0$–$9s^1S$	1–0	4054·711	4·34	22:	1·73	−2·91	−2·88	−2·83	
	$3p^1P^0$–$3d^1D$	1–2	8806·775	4·34	497	2·75	+0·43	+0·33	+0·08	
9	$3p^1P$–$4d^1D$	1–2	5528·418	4·34	300	2·72	−3·97	−0·25	−0·48	
11	$3p^1P^0$–$5d^1D$	1–2	4703·003	4·34	326	2·84	−1·71	−0·60	−0·40	
14	$3p^1P^0$–$6d^1D$	1–2	4351·921	4·34	283:	2·81	−1·67	−1·14	−0·62	
15	$3p^1P^0$–$7d^1D$	1–2	4167·277	4·34	200:	2·68	−1·77	−1·84	−1·16	
16	$3p^1P^0$–$8d^1D$	1–2	4057·515	4·34	197:	2·69	−1·91		−1·11	
	$4s^3S$–$4p^3P^0$	1–2	15025·17	5·11	538	2·55	+0·33	+0·33	−0·42	
22	$4s^3S$–$5p^3P^0$	1–2	7657·606	5·11	114	2·17	−1·12	−1·12	−1·22	
	$4s^3S$–$8p^3P^0$	1–2	5509·548	5·11	7·5	1·13	−2·38	−2·38	−2·70	(1)
		1–1, 0	5509·727	5·11	5·5	1·00	−2·47	−2·47	−2·83	
	$4s^1S$–$4p^1P^0$	0–1	17108·66	5·39	951	2·75	+0·13	+0·14	+0·31	
	$3d^1D$–$7p^1P^0$	2–1	8209·85	5·75	8·7	1·02	−3·63	−0·93	−2·20	
	$3d^1D$–$4f^1F^0$	2–3	12083·70	5·75	260	2·33	+0·53	+0·16	−0·10	
	$3d^1D$–$5f^1F^0$	2–3	9255·79	5·75	210	2·36	0·00	−0·24	−0·09	
28	$3d^1D$–$6f^1F^0$	2–3	8213·041	5·75	168	2·31	−0·35	−0·53	−0·36	
29	$3d^1D$–$7f^1F^0$	2–3	7691·569	5·75	126	2·21	−0·61	+0·10	−0·66	
30	$3d^1D$–$8f^1F^0$	2–3	7387·700	5·75	118	2·20	−0·83	−0·85	−0·70	
31	$3d^1D$–$9f^1F^0$	2–3	7193·183	5·75	60	1·92	−1·01	−0·74	−1·17	
33	$3d^1D$–$11f^1F^0$	2–3	6965·408	5·75	25	1·56	−1·31	−1·06	−1·64	
34	$3d^1D$–$12f^1F^0$	2–3	6894·89	5·75	6	0·94	−1·43	−1·17	−2·26	
	$3d^1D$–$13f^1F^0$	2–3	6841·19	5·75	8	1·07	−1·57	−1·28	−1·97	
	$3d^1D$–$14f^1F^0$	2–3	6799·05	5·75	1·5	0·34	−1·65	−1·38	−2·72	
	$4p^3P^0$–$4d^3D$	2–3, 2, 1	15766·02	5·93	525	2·52	+0·47	+0·48	−0·14	
		0–1	15740·71	5·93	260	2·22	−0·22	−0·22	−0·77	

	$4p^3P^0$–$7d^3D$	2–3, 2, 1	8717·833	5·93	104	2·08	−0·85	−0·84	−0·84
	$4p^3P^0$–$8d^3D$	2–3, 2, 1	8310·252	5·93	60	1·86	−1·07		−1·12
		1–2, 1	8305·617	5·93	34	1·61	−1·29		−1·39
	$4p^3P^0$–$10d^3D$	2–3, 2, 1	7881·67	5·93	9:	1·06	−1·42		−1·94
	$4p^3P^0$–$11d^3D$	2–3, 2, 1	7759·37	5·93	8	1·01	−1·57		−2·00
	$4p^3P^0$–$8s^3S$	2–1	8997·16	5·93	19	1·32	−1·79	−1·78	−1·40
	$4p^3P^0$–$9s^3S$	2–1	8473·663	5·93	10	1·07	−2·04	−2·03	−1·95
	$4p^3P^0$–$10s^3S$	2–1	8159·15	5·93	8·6	1·02	−2·24		−2·00
	$3d^3D$–$5f^3F^0$		10811·14	5·94	485	2·65	+0·48	+0·48	+0·38
	$3d^3D$–$6f^3F^0$		9414·95	5·94	264:	2·45	+0·08	+0·08	−0·12
39	$3d^3D$–$7f^3F^0$		8736·040	5·94	220	2·40	−0·21	−0·21	−0·28
40	$3d^3D$–$8f^3F^0$		8346·131	5·94	166	2·30	−0·44	−0·44	−0·66
41	$3d^3D$–$9f^3F^0$		8098·746	5·95	125:	2·19	−0·63	−0·63	−0·78
42	$3d^3D$–$10f^3F^0$		7930·819	5·95	41	1·71	−0·79		−1·31
43	$3d^3D$–$11f^3F$		7811·16	5·95	35	1·65	−0·93		−1·37
44	$3d^3D$–$12f^3F$		7722·64	5·95	15	1·30	−1·06		−1·73
	$3d^3D$–$15f^3F$		7560·54	5·95	<3	<0·6	−1·38		< −2·5
	$4p^1P^0$–$8s^1S$	1–0	10299·29	6·12	64	0·79	−2·07	−2·09	−2·13
	$4p^1P^0$–$11s^1S$	1–0	9004·92	6·12	2·2	0·39	−2·71		−2·50
	$4p^1P^0$–$6d^1D$	1–2	11522·25	6·12	31	1·43	−3·97	−0·65	−1·46
	$4p^1P^0$–$7d^1D$	1–2	10312·53	6·12	15	1·16	−2·50	−1·24	−1·74
	$4p^1P^0$–$9d^1D$	1–2	9273·44	6·12	9·2	1·00	−2·40		−1·93
	$4p^1P^0$–$11d^1D$	1–2	8837·05	6·12	3·1	0·54	−2·55		−2·50
	$4p^1P^0$–$12d^1D$	1–2	8707·14	6·12	3·6	0·62	−1·86		−2·42
	$5s^1S$–$6p^1P^0$	0–1	21459·17	6·51	30	1·15	−1·76	−1·24	−1·57
	$4d^1D$–$5f^1F^0$	2–3	24566·37	6·59	254	2·01	−0·20	−1·49	−0·27
	$4d^1D$–$7f^1F^0$	2–3	15954·51	6·59	112	1·85	−0·73	+0·49	−0·84
	$4d^3D$–$6f^3F^0$		22808·11	6·72	348	2·18	+0·40	+0·40	−0·12
	$4d^3D$–$9f^3F^0$		16365·02	6·72	186	2·06	−0·43	−0·43	−0·55
	$5p^3P^0$–$8s^3S$	2–1	21225·80	6·72	24	1·05	−1·07	−1·33	−1·50

Notes:

(1) Swensson & Risberg (1966) proposed for λ 5509·548 the identification ΔJ = 1–2, 1, 0. An examination of the separations in the np^3P term indicates that two separate lines ΔJ = 1–2 and 1–1, 0 are predicted. The present identification for the latter is believed to be new.

: Denotes uncertain measurement.

* Column (a) gives the log gf calculated assuming LS coupling line strengths and coulomb approximation radial integrals. Column (b) gives the log gf obtained from intermediate coupling calculations and STFD radial integrals. Column (c) gives the astrophysical log gf values.

systematically too small owing to the disappearance of their weak but extensive wings in the noise in either photographic or photoelectric tracings. The present assumption of the standard damping constants is considered a suitable compromise pending detailed line profile studies and further study of the apparent necessity for an increase in these standard damping constants.

2.2 *The Mg* II *spectrum*

2.2.1 *Introduction.* The selection of Mg II lines was based on the laboratory spectrum analysis by Risberg (1955). In a comparison of laboratory and solar data, Risberg listed 11 lines as present in the solar spectrum for $\lambda \geq 4000$ Å. The predicted equivalent widths for two lines do not exceed 0·2 mÅ and it is suggested that their identification with Fraunhofer lines results from a chance wavelength coincidence: the lines are at 10 392·23 and 10 092·16 Å. The lines at 9244·27, 4481·14, and 4481·34 Å are seriously blended and are excluded from the abundance analysis. The latter doublet has been used by several authors but owing to the presence of a strong Ti I line at 4481·28 Å, accurate line profile studies and a careful analysis of the complete blend are necessary to deduce an accurate abundance. Such observations are not available at this time. The line list in Table III gives details of the six lines chosen from Risberg's list as well as two additional identifications for lines identified on the Delbouille & Roland Atlas (1963). The line at 9632·44 Å is a new identification.

2.2.2 *Oscillator strengths.* There are no experimental measurements of oscillator strengths for the transitions listed in Table III. Fortunately, the coulomb approximation radial integrals with the LS-coupling line strengths may be applied with some confidence to the Mg II transitions. The resulting oscillator strengths are given in Table III. It is of interest that computations (Warner 1968b) which make an allowance for the effect of configuration mixing by spin–orbit interaction differ from the adopted values by less than 1 per cent.

2.2.3 *The magnesium abundance.* The equivalent widths for the Mg II lines were measured off the Delbouille & Roland Atlas (1963). Supplementary measurements for several lines were obtained from the literature. The strongest line at 9218 Å, which is a blend of Mg II and two CN lines, is not included in the derivation of the mean abundance but it is consistent with the mean value (see footnote (1) to Table III). A composite curve of growth is shown in Fig. 1. Assigning equal weight to the remaining seven lines the mean abundance is given by [Mg] = +0·1(with a total range of ±0·09 about the mean. The small range is probably entirely attributable to errors of measurement affecting the equivalent widths and would imply that confidence may be placed in the theoretical oscillator strengths.

However, it has proved necessary to inject a cautionary note into the apparently satisfactory conclusion represented by the curve of growth in Fig. 1. de Jager & Neven (1967) have published line profiles for the Mg II lines at 10 914·25 and 10 951·82 Å.* The calculated and observed profiles for the former line at the centre of the solar disk are compared in Fig. 2. Two calculated profiles are shown; one normalized to the observed equivalent width and the other to the central intensity

* de Jager & Neven quote the wavelengths as 10 914·20 and 10 949·40 Å. There is no line of the observed intensity at this latter wavelength but it is assumed that their observations refer to the line at 10 951·82 Å.

TABLE III

Mg II *lines in the solar spectrum*

RMT No.	Multiplet	ΔJ	$\lambda_\odot$ (Å)	χ (eV)	log gf	W_λ (mÅ)	$\log \frac{W_\lambda}{\lambda}+7$	[Mg]	Remarks*
1	$4s^2S$–$4p^2P$	$\frac{1}{2}$–$\frac{3}{2}$	9218·251	8·65	+0·26	74			L (1)
3	$3d^2D$–$4p^2P$	$\frac{5}{2}$–$\frac{3}{2}$	10914·25	8·86	+0·03	55	1·70	+0·23	55L, 47Mi, 74deJN
		$\frac{3}{2}$–$\frac{1}{2}$	10951·82	8·86	−0·23	32	1·47	+0·10	L (2)
7	$4p^2P$–$5s^2S$	$\frac{1}{2}$–$\frac{1}{2}$	8213·85	10·00	−0·28	4·9	0·78	+0·17	4·9L, 10RRT, (3)
8	$4p^2P$–$4d^2D$	$\frac{3}{2}$–$\frac{5}{2}$	7896·378	10·00	+0·65	27	1·53	+0·27	27L, 24Mi, 28RRT
		$\frac{1}{2}$–$\frac{3}{2}$	7877·059	10·00	+0·39	17	1·33	+0·22	17L, 20RRT
15	$4d^2D$–$5f^2F$	$\frac{5}{2}$–$\frac{7}{2}$	9631·87	11·57	+0·66	3·1	0·51	+0·24	
		$\frac{3}{2}$–$\frac{5}{2}$	9632·44	11·57	+0·50	1·6	0·22	+0·10	(4)

* Mi ≡ Mitchell (1959).

Notes:

(1) The measured W_λ includes the CN lines (1, 0) $R_1(26)$ and $R_2(28)$ at 9218·237 Å. Their predicted (unblended) W_λ = 14 mÅ. Therefore, the Mg II contribution is $74 > W_\lambda > 60$ or $+0{\cdot}30 > [\mathrm{Mg}] > +0{\cdot}09$.

(2) de Jager & Neven (1967) probably measured this line and obtained W_λ = 42 mÅ but they give the wavelength as 10 949·40 and there is no Fraunhofer line at this wavelength.

(3) According to the RRT, an atmospheric H_2O line is a contributor. This would account for the large range in the W_λ measurements quoted in the Remarks column.

(4) New identification.

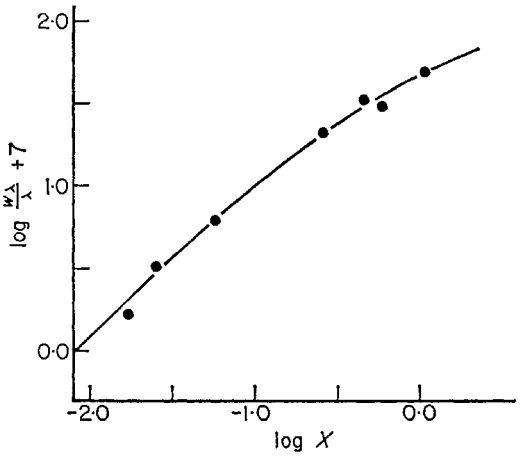

FIG. 1. *The solar curve of growth for Mg* II.

The striking result is the gross disagreement between computed and observed profiles which is especially noticeable on account of the extensive wings. Previous discussion (Section 2.1.4) hinted that an increase in the standard damping constant by a factor of 2 may be required. This increase would result in only minor changes in the computed profiles.

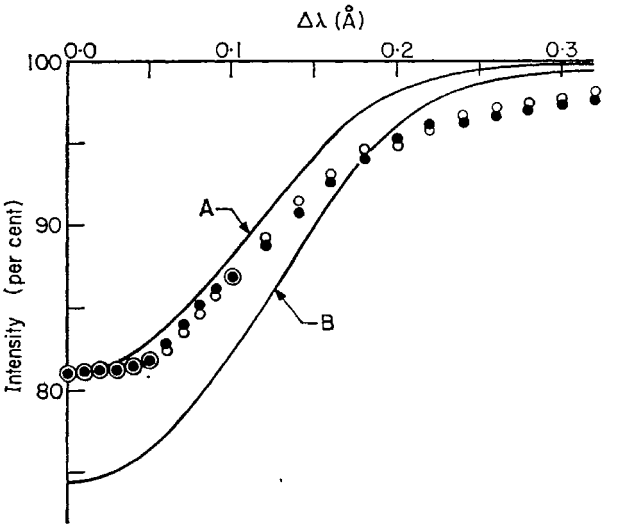

FIG. 2. *Line profiles for the Mg* II *line at* 10 914·25 *Å. The observed profile for the centre of the disk is taken from the observations of de Jager & Neven* (1967)*: filled circles denote the red wing and open circles the blue wing. Predicted profiles are shown by the solid lines: profile A is fitted to the observed central intensity and B to the observed equivalent width.*

The discrepancy between observed and computed profiles was unexpected Possible changes in the assumed microturbulent velocity field will affect the latter profiles to only a minor extent. More fundamental changes in the adopted model atmosphere appear to be necessary. In particular, qualitative considerations suggest that with the introduction of a two or three stream model with convective motions in the deeper layers amounting to about 3 km s^{-1}, the predicted profiles would have extensive wings as is observed. A detailed theoretical and observational test of this proposal is in progress.

The derivation of the recommended value for the magnesium abundance is hampered by the discrepancy between the Mg I and Mg II solutions:

$$\text{from 15 Mg I lines: [Mg]} = -0{\cdot}04 \pm 0{\cdot}03$$

$$\text{from 7 Mg II lines: [Mg]} = +0{\cdot}19 \pm 0{\cdot}02.$$

The significantly smaller total spread in the Mg II solutions for individual lines would suggest that greater weight be assigned to the latter result. However, the discrepancy in the Mg II line profiles would suggest that this assignment is a little premature. A compromise solution is adopted and equal weight is assigned to the Mg I and Mg II solutions. The mean abundance is, therefore,

$$[\text{Mg}] = +0{\cdot}08 \text{ or } \log N(\text{Mg}) = 7{\cdot}48.$$

It is hoped that the study in progress will result in an explanation of the Mg II line profiles and that this may reduce the apparent discrepancy between the abundances derived from the independent analyses of the first and second spectra.

3. *Calcium*

3.1 *The Ca I spectrum*

3.1.1 *Introduction.* The Ca I spectrum has been used in all attempts to derive the calcium abundance. Identified lines of Ca I are numerous and a good selection of unblended lines is available. The principal difficulty concerns the oscillator strengths and, in particular, the correct normalization factor for the accurate and extensive measurements of relative oscillator strengths.

3.1.2 *Oscillator strengths.* The primary aim in this discussion is to present a new attempt to normalize onto an absolute scale the accurate relative oscillator strength measurements made by Olsen, Routly & King (1959). Earlier work (for example Müller & Mutschlecner 1964) combined a theoretical calculation of the absolute oscillator strength of the resonance transition λ 4227 with a measured ratio for the relative strengths of the intercombination line λ 6572 and λ 4227 so enabling the relative measurements which included λ 6572 to be placed on an absolute scale. A different method is adopted here.

The resonance line is too heavily blended in the solar spectrum to be reliably analysed. However, since the oscillator strength for the intercombination line is obtained using measurements of the oscillator strength for the resonance line, a brief discussion of these measurements must be given.

The oscillator strength for the resonance transition $4s^2\ {}^1S_0$–$4s4p\ {}^1P_1$ at 4227 Å has been accurately determined from lifetime measurements using the Hanle effect with the following results:

Smith & Gallagher (1966)	$f_{4227} = 1{\cdot}74 \pm 0{\cdot}06$
Lurio, de Zafra & Goshen (1964)	$= 1{\cdot}79 \pm 0{\cdot}06$
Hulpke, Paul & Paul (1964)	$= 1{\cdot}72 \pm 0{\cdot}04.$

A mean value $f_{4227} = 1{\cdot}74 \pm 0{\cdot}02$ is adopted. Hook measurements by Ostrovskii & Penkin (1961b) give $f_{4227} = 1{\cdot}49 \pm 0{\cdot}04$ which differs by about 25 per cent from the accurate determination based on the measured lifetimes. The discrepancy is probably attributable to an error in the adopted vapour pressure for calcium.

Indeed, it would now be preferable to reverse the analysis of the hook experiment in order to derive the vapour pressure.

Trefftz (1951) calculated f_{4227} using Hartree–Fock wave functions and with allowance for configuration interaction. The dipole-length and dipole velocity formulations yielded $f_{4227} = 1{\cdot}737$ and $1{\cdot}223$ respectively. The geometric mean ($f_{4227} = 1{\cdot}458$) is the result usually attributed to Trefftz. However, since the dipole length formulation gives most weight to the outer part of the wavefunction, it should be considered the more reliable approach. The agreement with experiment is then remarkable. The oscillator strength has been recomputed using the wavefunctions calculated by the STFD method (Warner 1968a) and adopting Trefftz's calculations for the compositions of the $4s^2\,{}^1S_0$ and $4s4p\,{}^1P_1$ states. The result $f_{4227} = 1{\cdot}789$ is in close agreement with the experimental determination based on the Hanle effect.

No direct measurement has been reported for the absolute oscillator strength of the intercombination line $4s^2\,{}^1S_0$–$4s4p\,{}^3P_1$ at 6572 Å. Ostrovskii & Penkin (1961a) measured the ratio $f_{6572}/f_{4227} = 2{\cdot}79 \times 10^{-5}$ using the hook method. This result is independent of errors in the adopted vapour pressure for calcium. Their result should be considered an improvement on the value $3{\cdot}0 \times 10^{-5}$ found earlier by Prokofiev (1928) and adopted by Müller & Mutschlecner (1964). The new ratio measurement and the adopted mean value for f_{4227} give $f_{6572} = 4{\cdot}85 \times 10^{-5}$.

There are available two extensive and accurate series of relative oscillator strengths for Ca I (Olsen *et al.* 1959; Ostrovskii & Penkin 1961a). The relative agreement of the two series (excluding the inter-combination line) is excellent; any systematic difference between the two series does not exceed 10 to 15 per cent which is less than the quoted errors of measurement. In the experiments performed by Olsen *et al.* using the King furnace absorption technique, the resonance line 4227 Å was omitted because of its great strength but the intercombination line 6572 Å was included.

With the above determined values of f_{4227} and f_{6572}, it would appear straightforward to place these relative measurements onto an absolute scale. However, two points demand special consideration. Firstly, the ratio f_{6572}/f_{4227} is difficult to determine with high accuracy because of the great difference in oscillator strength between the two lines. Secondly, the connection between 6572 Å which originates from the ground state ($\chi = 0$ eV) and the other multiplets, which have $\chi \geq 1{\cdot}88$ eV (for the lines considered in the abundance analysis) is rendered uncertain owing to the dependence of the connection on the temperature determination in the absorption tube. The latter uncertainty is probably the more important and the comparison of the two series of relative measurement is instructive. The ratio f_λ/f_{6572} is systematically larger by 0·15 dex in the data of Olsen *et al.* than that given by Ostrovski & Penkin. Therefore, if the result $f_{6572} = 4{\cdot}86 \times 10^{-5}$ is adopted, the relative oscillator strength of Olsen *et al.* should be multiplied by the factor $1{\cdot}80 \times 10^{-5}$ in order to place them on an absolute scale. On the other hand, if the ratio between 6572 Å and the other lines as determined by Ostrovskii & Penkin is preferred, the normalization factor for the data of Olsen *et al.* is reduced to $1{\cdot}28 \times 10^{-5}$. This difference in the normalization factor plus the uncertainty in the ratio f_{6572}/f_{4227} is a direct measure of the uncertainty in the calcium abundance determination.

In an attempt to reduce the uncertainty inherent in the above method of normalization, the possibility of a calibration from theoretical oscillator strength for selected transitions was explored.

The Ca I spectrum, although essentially a two electron spectrum, is made very complex owing to configuration interaction. In addition, certain of the low-lying states are extremely non-coulombic so that accurate wavefunctions are required for the calculation of the oscillator strengths. A complete treatment of the Ca I spectrum is beyond the scope of the present paper. However, it is possible to select certain transitions for which a close approach to LS-coupling may be demonstrated from a discussion of the Ca I term structure.

Among the even parity terms, there are $4s^2$, $4sns$ giving rise to $^3S_1$ and $^1S_0$, $4snd$ giving $^1D_2$ and $^3D_{1,2,3}$, and $4p^2$ giving $^3P_{0,1,2}$, $^1S_0$ and $^1D_2$. The first term in each series has a low energy. Terms from $3d5s$, $3d^2$ and $3dnd$ occur at somewhat higher energies. Miss Trefftz's calculations show that the $^1S_0$ terms of $4s^2$ and $4p^2$ are strongly mixed and it is anticipated that all of the $4sns$ $^1S_0$ levels will also be mixed with them. Similarly, and in analogy with the Mg I spectrum (Warner 1968c), the $4snd$ $^1D_2$ levels will be strongly mixed both with themselves and with $4p^2$ $^1D_2$. The $4snd$ ^3D terms are expected to be more pure but the possibility of some mixing with the $3d5s$ ^3D and $3dnd$ ^3D terms cannot be ruled out. It is to be noted that the $^3S_1$ level arises only from the $4sns$ configurations and mixing between the various ns levels is not expected to be important.

The terms of odd parity include $4snp$ giving rise to ^3P and ^1P terms and the low-lying $3dnp$, which also provide ^3P and ^1P among others. The mixing is expected to be greatest for singlet terms; for example, $3d4p$ ^1P lies between $4s4p$ ^1P and $4s5p$ ^1P and the latter is quite clearly perturbed upwards from the $4s5p$ ^3P term, and indeed, Miss Trefftz's calculations provide quantitative estimates for the mixing. On the other hand, the $4s4p$ ^3P and $3d4p$ ^3P terms are widely separated and mixing is not expected to be important. Spin–orbit mixing in $4s4p$ is also not large; from the ratio f_{4226}/f_{6572} it can be shown that the admixture of $^1P_1$ into $^3P_1$ is less than 0·7 per cent. However, $4s5p$ $^3P^0$ is very close to $3d4p$ ^3P and is clearly perturbed.

The conclusion, which is drawn from this discussion of the term diagram, is that the only multiplets for which the LS coupling multiplet strengths may be confidently applied are $4s4p$ ^3P–$4sns$ ^3S. Fortunately, Olsen *et al.* observed six such multiplets. The total gf values for these multiplets, which were calculated from STFD wave functions, are given in Table IV. The total relative gf-values as measured by Olsen *et al.* are also tabulated and the ratio of the observed to calculated values is given in the final column.

TABLE IV

Comparison of measured and theoretical f-values for Ca I

Multiplet	λ(Å)	gfSTFD	gfREL	gfSTFD/gfREL × 10^{-4}
$4p^3P$–$5s^3S$	6120	1·066	$8{\cdot}39 \times 10^4$	7·87
–$6s^3S$	3960	0·1441	$1{\cdot}51 \times 10^4$	10·49
–$7s^3S$	3470	0·0513	$5{\cdot}25 \times 10^3$	10·20
–$8s^3S$	3270	0·02492	$3{\cdot}14 \times 10^3$	12·59
–$9s^3S$	3170	0·01445	$1{\cdot}71 \times 10^3$	12·11
–$10s^3S$	3105	0·008850	$1{\cdot}01 \times 10^3$	11·42

It can be seen that despite the large wavelength range covered by the $4p$–ns transitions, the ratio of the observed to calculated gf-values is sensibly constant. The first member of the series at 6120 Å gives the lowest value for the ratio. This could be interpreted to suggest that for $\lambda > 6000$ Å the oscillator strengths given

by Olsen *et al.* are systematically too small. The comparison of the results for the ratio f_λ/f_{6572} as measured by Ostrovskii & Penkin and by Olsen *et al.* would support this suggestion.

The average of the ratios given in Table I, giving the first series member only half weight, is $11{\cdot}00 \times 10^4$ and corresponds to a reduction factor of $9{\cdot}10 \times 10^{-6}$ to be applied to the relative oscillator strengths of Olsen *et al.* This is a factor of 1·41 smaller than the normalization factor from a combination of the accurate oscillator strengths for 4227 Å and the ratio of this to the other lines given by Ostrovskii & Penkin. If this difference is interpreted as a temperature effect, it would imply that the absorption tube used by Ostrovskii & Penkin was some 120°K hotter than their measured value of 2800°K.

In this study of the solar Ca I lines, the relative *gf*-values of Olsen *et al.* are adopted with a normalization factor of $9{\cdot}10 \times 10^{-6}$. For the intercombination line 6572 Å the experimental determination (see above) $f_{6572} = 4{\cdot}86 \times 10^{-5}$ is adopted.

3.1.3 *Ca I lines in the solar spectrum.* The Ca I lines employed in the abundance analysis are listed in Table V. The selection is made from the line list given by Olsen *et al.* and includes all lines at $\lambda \geq 4000$ Å for which an equivalent width measurement is available from photoelectric tracings obtained from the McMath–Hulbert Atlas. These equivalent widths were listed by Müller & Mutschlecner (1964) and by Holweger (1967).

The line list includes few weak lines so that a correct evaluation of the damping constants is essential. The radiative component was estimated from the available oscillator strength measurements. The Stark component is expected to be unimportant; a constant value $\Delta\nu/E^2 = 5 \times 10^{-12}$ was assumed for all multiplets. The van der Waals contribution was computed from mean square radii obtained from the STFD wavefunctions. The consequences of an error in the damping constant increases with increasing strength of the line. For a typical multiplet (RMT 20) the effect of a uniform increase in damping constant by a factor of 2 was determined. At $\log W_\lambda/\lambda + 7 = 2{\cdot}4$, the abundance error amounts to −0·18 dex, and decreases to −0·10 and −0·04 for $\log W_\lambda/\lambda + 7 = 2{\cdot}3$ and 2·2 respectively.

The results for the calcium abundance obtained from the individual lines are given in the final column of Table V. The mean abundance from all 43 lines is [Ca] = +0·18 ± 0·03. A closer analysis suggests a total absence of systematic dependence of the abundance on wavelength or equivalent width. The 14 lines with $\lambda \leq 5000$ Å give [Ca] = +0·17 and the 29 lines at $\lambda \geq 5000$ Å give [Ca] = +0·19. For $\lambda \geq 5000$ Å, the following results are obtained from a breakdown according to equivalent width:

$$\log \frac{W_\lambda}{\lambda} + 7 \leq 2{\cdot}20 \qquad [\mathrm{Ca}] = +0{\cdot}16\ (10)$$

$$2{\cdot}20 \leq \leq 2{\cdot}40 \qquad = +0{\cdot}16\ (15)$$

$$\leq 2{\cdot}40 \qquad = +0{\cdot}41\ (4)$$

where the number of lines in each group is given in parentheses. The apparently discordant result for the strongest lines is attributable to inclusion of two lines from multiplet (3) (see Table II) but the reason for the large deviations from the mean obtained from these lines is unknown. A similar breakdown for the group with $\lambda \leq 5000$ Å gives for the eight lines with $\log W_\lambda/\lambda + 7 \geq 2{\cdot}40$, the abundance [Ca] = +0·13 in good agreement with the weaker lines. Therefore, it is possible that the

TABLE V

Ca I *lines in the solar spectrum*

RMT No.	Multiplet	ΔJ	$\lambda_\odot$ (Å)	χ (eV)	log gf	W_λ (mÅ)	log $\frac{W_\lambda}{\lambda}+7$	[Ca]
1	$4s^2\ ^1S$–$4p\ ^3P^0$	0–1	6572·795	0·00	−4·31	25	1·58	+0·07
3	$4p\ ^3P^0$–$5s\ ^3S$	2–1	6162·180	1·90	−0·39	294	2·68	+0·69
		1–1	6122·226	1·89	−0·57	210	2·54	+0·47
		0–1	6102·727	1·88	−1·05	130	2·33	+0·22
4	$4p\ ^3P^0$–$4d\ ^3D$	2–3	4454·793	1·90	+0·10	187	2·62	−0·15
		2–2	4455·893		−0·72	129	2·46	+0·10
		2–1	4456·627		−1·79	75	2·23	+0·34
		1–2	4434·967	1·89	−0·26	180	2·61	+0·18
		1–1	4435·688		−0·69	138	2·49	+0·18
		0–1	4425·444	1·88	−0·56	149	2·53	+0·19
5	$4p\ ^3P^0$–$4p^2\ ^3P$	2–1	4318·659	1·90	−0·40	129	2·48	+0·03
		1–2	4283·014	1·89	−0·39	147	2·53	+0·25
		0–1	4289·372	1·88	−0·52	139	2·51	+0·29
18	$3d\ ^3D$–$3d4p\ ^3F^0$	3–4	6439·083	2·53	−0·08	171	2·42	+0·42
		3–3	6471·668		−0·90	90	2·15	+0·14
		2–2	6499·654	2·52	−1·04	84	2·11	+0·16
		1–2	6493·788		−0·43	124	2·28	+0·17
19	$3d\ ^3D$–$3d4p\ ^1D^0$	2–2	6455·605	2·52	−1·54	53	1·92	+0·24
		1–2	6449·820		−0·82	101	2·19	+0·18
20	$3d\ ^3D$–$5p\ ^3P^0$	3–2	6169·564	2·53	−0·72	113	2·26	+0·19
		2–2	6161·295	2·52	−1·31	61	2·00	+0·13
		2–1	6169·044		−0·93	92	2·17	+0·14
		1–1	6163·754		−1·45	57	1·97	+0·21
		1–0	6166·440		−1·30	67	2·04	+0·20
21	$3d\ ^3D$–$3d4p\ ^3D^0$	3–3	5588·764	2·53	+0·14	151	2·43	+0·05
		3–2	5601·286		−0·54	118	2·32	+0·26
		2–3	5581·979	2·52	−0·54	96	2·24	−0·06
		2–2	5594·471		−0·09	131	2·37	+0·07
		1–2	5590·126		−0·66	93	2·22	−0·02
		1–1	5598·491		−0·23	124	2·35	+0·08
22	$3d\ ^3D$–$3d4p\ ^3P^0$	2–1	5265·560	2·52	−0·29	129	2·39	+0·24
		1–2	5260·390		−1·70	31	1·76	+0·09
		1–1	5261·708		−0·71	102	2·29	+0·23
23	$3d\ ^3D$–$4f\ ^3F^0$	1–2	4578·559	2·52	−0·84	83	2·26	+0·06
25	$3d\ ^3D$–$4f\ ^3F^0$	2–3	4094·938	2·52	−0·89	100	2·39	+0·37
32	$3d\ ^1D$–$3d4p\ ^1P^0$	2–1	6717·687	2·71	−0·80	110	2·21	+0·48
33	$3d\ ^1D$–$3d4p\ ^1F^0$	2–3	5349·469	2·71	−0·37	100	2·27	+0·01
34	$3d\ ^1D$–$5p\ ^1P^0$	2–1	5041·619	2·71	−0·48	104	2·32	+0·08
36	$3d\ ^1D$–$6p\ ^1P^0$	2–1	4526·933	2·71	−0·63	92	2·31	+0·09
37	$3d\ ^1D$–$5f\ ^1F^0$	2–3	4355·093	2·71	−0·63	100	2·36	+0·22
39	$3d\ ^1D$–$6f\ ^1F^0$	2–3	4108·532	2·71	−0·93	82	2·30	+0·27
47	$4p\ ^1P^0$–$4p^2\ ^1D$	1–2	5857·459	2·93	+0·17	143	2·39	+0·35
48	$4p\ ^1P^0$–$6s\ ^1S$	1–0	5512·989	2·93	−0·48	91	2·22	+0·06

discordant result for RMT 3 may be attributable to errors in the measured equivalent widths. It is of interest that with the exception of RMT 3 there is no strong evidence for the two-fold increase in damping constant which was discussed in Section 2.1.4.

The abundance [Ca] = $+0{\cdot}18 \pm 0{\cdot}03$ is adopted as the mean result based on the Ca I lines. The recommended abundance is presented after the discussion on the Ca II lines. This revision is +0·29 dex larger than the value obtained by Müller & Mutschlecner (1964). This difference is attributable primarily to the revision

in the absolute scale of the Ca I relative oscillator strengths with smaller revisions introduced by the use of a more complete treatment of the damping constants and the adoption of an alternative model atmosphere.*

3.2 *The Ca II spectrum*

3.2.1 *Introduction.* The Ca II lines present in the solar spectrum were listed by Edlén & Risberg (1956). The selection of lines for an abundance analysis was made from their list. Details for 18 lines are given in Table VI. The Ca II H and K lines and the infrared triplet $3d^2D$–$4p\ ^2P^0$ have not been considered. These lines, which are very strong, are almost certainly formed under non-LTE conditions (Dumont 1967). Although it appears feasible to attempt an analysis of their line profiles in the wings, which are formed in regions of the atmosphere in which non-LTE effects are small or negligible, the discussed uncertainties concerning the damping constant diminishes the present usefulness of this analysis. It should be pointed out that, except for isolated analyses of the H and K lines on the infrared triplet, Ca II spectrum has not been previously considered for an abundance analysis.

TABLE VI

Ca II lines in the solar spectrum

RMT No.	Multiplet	ΔJ	$\lambda_\odot$ (Å)	χ (eV)	log gf	W_λ (mÅ)	log $\frac{W_\lambda}{\lambda}$	[Ca]	Notes
5	$5s^2S$–$5p^2P$	$\frac{1}{2}$–$\frac{3}{2}$	11839·00	6·47	+0·29	196	2·22	+0·34	(1)
		$\frac{1}{2}$–$\frac{1}{2}$	11949·77		−0·01	135	2·05	+0·15	
	$4d^2D$–$4f^2F$	$\frac{5}{2}$–$\frac{5}{2}$, $\frac{7}{2}$	8927·392	7·05	+0·82	132	2·17	+0·18	
		$\frac{3}{2}$–$\frac{5}{2}$	8912·101		+0·74	118	2·12	+0·13	
12	$5p^2P$–$6s^2S$	$\frac{3}{2}$–$\frac{1}{2}$	9931·45	7·51	+0·06	48	1·68	+0·26	
		$\frac{1}{2}$–$\frac{1}{2}$	9854·66	7·50	−0·26	30	1·48	+0·26	
14	$5p^2P$–$7s^2S$	$\frac{3}{2}$–$\frac{1}{2}$	5307·231	7·51	−0·88	7	1·12	+0·18	
		$\frac{1}{2}$–$\frac{1}{2}$	5285·262	7·50	−1·18	3	0·75	+0·10	
13	$5p^2P$–$5d^2D$	$\frac{3}{2}$–$\frac{5}{2}$	8248·802	7·51	+0·57	70	1·93	+0·20	
		$\frac{3}{2}$–$\frac{3}{2}$	8254·681		−0·38	17	1·31	+0·18	
		$\frac{1}{2}$–$\frac{3}{2}$	8201·695	7·50	+0·31	51	1·79	+0·17	(2)
15	$5p^2P$–$6d^2D$	$\frac{3}{2}$–$\frac{3}{2}$	5021·151	7·51	−1·23	4	0·90	+0·37	
		$\frac{1}{2}$–$\frac{3}{2}$	5001·472	7·50	−0·53	20	1·60	+0·25	
	$4f^2F$–$5g^2G$		9890·67	8·44	+1·27	74	1·87	+0·21	
19	$4f^2F$–$6g^2G$		6456·865	8·44	+0·43	17	1·42	+0·13	(3)
20	$4f^2F$–$7g^2G$		5339·217	8·44	−0·05	3	0·75	−0·27	(4)
	$4f^2F$–$5d^2D$	$\frac{7}{2}$–$\frac{5}{2}$	21389·08	8·44	+0·17	33	1·19	+0·02	
		$\frac{5}{2}$–$\frac{3}{2}$	21428·72		+0·11	30	1·15	+0·03	

Notes:

(1) Babcock & Moore (1947) attribute this line to Ti. The Ti line may account for the large value for [Ca] obtained for this line.
(2) In the RRT an unclassified atmospheric (probably H_2O) line is given as a contributor.
(3) According to the RRT, this line is a blend of an Fe Ip line and the Ca II line. The former is almost certainly a minor contributor.
(4) See text for discussion of equivalent width.

*A recent determination (Karstensen, F. & Schramm, J., 1968. *Z. Astrophys.*, **68**, 214) of the radiative lifetime of the $4f\ ^1F^0$ level in Ca I gives log $gf = -0{\cdot}32 \pm 0{\cdot}02$ for λ4878 ($3d\ ^1D$–$4f\ ^1F^0$). This is in good agreement with the value log $gf = -0{\cdot}26$ deduced from the relative f-values of Olsen *et al.* (1959) with the normalization advocated in Section 3.1.2 of this paper.

3.2.2 *Oscillator strengths.* There are no experimental oscillator strength measurements for the transitions listed in Table VI. Fortunately, since the Ca II spectrum is a one-electron spectrum, coulomb approximation radial integrals with LS coupling line strengths are likely to prove satisfactory. The oscillator strengths for all except the $4f$–ng transitions were taken from Warner (1968b) and include allowance for the effect of spin–orbit interaction. For the s–p and p–d transitions, the introduction of spin–orbit interaction changes the computed oscillator strengths by less than 0·02 dex. The corrections to the oscillator strengths for d–f transitions are larger and differences up to 0·10 dex are introduced.

3.3.3 *The Ca abundance.* The composite curve of growth for the 19 Ca II lines is given in Fig. 3. The illustrated curve is drawn for $\lambda = 11\,900$ Å and $\chi = 6{\cdot}47$ eV. The small differences in shape for the curves of growth for other wavelengths and excitation potentials are not illustrated in Fig. 3 but were taken into account in the deviation of the abundances which are listed in the penultimate column of Table VI. In Fig. 3, the most divergent point is that of 5334 Å $4f$–$7g$, which is apparently a factor of 3 weaker than predicted on the basis of the computed oscillator strength and the revized abundance. However, the upper (7^2G) level

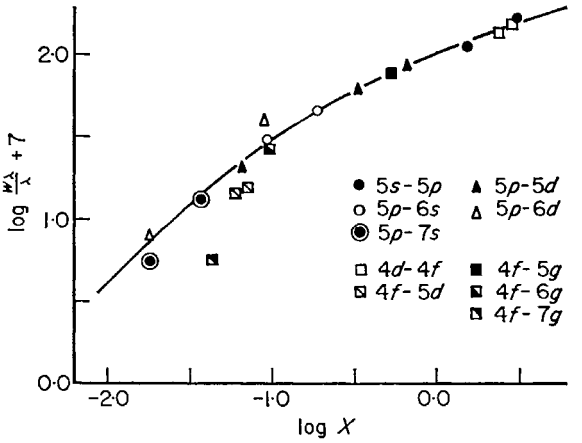

FIG. 3. *The solar curve of growth for Ca* II.

has a mean square radius ~1800 atomic units and is only 53 cm^{-1} distant from 7^2F. Consequently the damping constant for the transition $4f$–$7g$ is very large and the profile should be of almost pure dispersion type (*cf.* high level transitions in Na I, Lambert & Warner 1968a). As the Ca II 5339 Å line lies on the wing of the strong Fe I line at 5340 Å and the region is generally depressed in the Utrecht Atlas, we consider it likely that the extensive wings have been entirely lost and our quoted equivalent width of 3 mÅ may be a severe underestimate. In order to agree with our Ca abundance, this line should have an equivalent width of ~7–9 mÅ. We have omitted λ 5340 from the derivation of the mean abundance.

The mean abundance with equal weights assigned to the remaining 17 lines is

$$[\mathrm{Ca}] = +0{\cdot}18 \pm 0{\cdot}03.$$

Detailed results according to equivalent width are

$\log W_\lambda/\lambda + 7 \geq 1{\cdot}9$	$[\mathrm{Ca}] =$	$+0{\cdot}20 \pm 0{\cdot}03$ (5)
$1{\cdot}6 \leq \quad \leq 1{\cdot}9$		$+0{\cdot}22 \pm 0{\cdot}02$ (4)
$\leq 1{\cdot}6$		$+0{\cdot}16 \pm 0{\cdot}04$ (8)

where the number of lines in each group is given in parentheses. The absence of a detectable dependance on equivalent width and the small range in results from individual lines suggests that the mean value is well determined.

A residual element of doubt remains. Line profile studies for typical Mg II (Section 2.2.3) and Sr II (Section 4.3.3) lines suggests that the simple model atmosphere calculations fail to predict satisfactorily the observed line profiles. Profiles for Ca II lines other than the H and K or infrared triplet are not available in the literature but may be expected to show the same discrepancies between the observed and predicted profiles. Observations of lines in Table VI would be of interest.

The analyses of the Ca I and Ca II spectra provide results for the calcium abundance which are in excellent agreement; both analyses yielding [Ca] = +0·18 with an rms uncertainty of about ±0·03. The abundance which is adopted as the result of this investigation, must be

$$[\mathrm{Ca}] = +0{\cdot}18 \text{ or } \log N(\mathrm{Ca}) = 6{\cdot}33.$$

The true uncertainty is difficult to estimate; it is certainly greater than the rms uncertainty. The agreement between the Ca I and Ca II might be interpreted as evidence that the model atmosphere errors are small or unimportant relative to these analyses.

4. *Strontium*

4.1 *Introduction.* The strontium abundance derived by GMA was based on the resonance line and the line 4161 Å of Sr II. Eleven weak lines of Sr I were discussed but the best available oscillator strengths for these lines suggested an abundance which was a factor 3 or even 5 greater than that obtained from the resonance line. The present opportunity is taken to rediscuss the Sr I and Sr II spectra using the improved oscillator strengths and equivalent width measurements which are now available for some of these lines.

4.2 *The Sr I spectrum*

4.2.1 *Oscillator strengths.* An accurate determination for the oscillator strength of the resonance line $5s^2\ {}^1S_0$–$5s5p\ {}^1P_1$ at 4607·3 Å is now available from lifetime measurements using the Hanle effect. Lurio, de Zafra & Goshen (1964) give $gf = 1{\cdot}92 \pm 0{\cdot}06$ and Hulpke, Paul & Paul (1964) obtain $gf = 2{\cdot}09 \pm 0{\cdot}09$. A straight mean of $gf = 2{\cdot}00$ is adopted.

Measurements made by the hook method give a smaller result: $gf = 1{\cdot}54 \pm 0{\cdot}05$ according to Ostrovskii & Penkin (1961b). However, such measurements require a knowledge of the vapour pressure of strontium. The discrepancy between the results for the two methods indicates that the assumed vapour pressures were systematically in error.

A theoretical estimate for the oscillator strength is obtained from wavefunctions calculated from the STFD method and line strengths obtained from intermediate coupling calculations (Warner 1968a). The result of $gf = 2{\cdot}14$ is in reasonable agreement with the above mean result from the lifetime measurements.

The possibility was examined of placing relative measurements of Sr I oscillator strengths onto an absolute scale by adopting an analogous procedure to that employed for Ca I. However, the new normalization does not reduce significantly

the discrepancy referred to in Section 4.1 between the excited Sr I lines and the resonance line and a summary of the method must suffice.

An inspection of the Sr I term diagram suggests that the only multiplets for which the LS coupling multiplet strengths can be confidently applied are $5s5p\ ^3P$–$5sns\ ^3S$. Both Penkin & Shabanova (1965) and Eberhagen (1955) give measurements for $5p\ ^3P$–$6s\ ^3S$ and $5p\ ^3P$–$7s\ ^3S$. The latter author discussed the normalization to an absolute scale; GMA give an outline of the method. The ratio of the experimental (Eberhagen 1955) to the theoretical oscillator strengths from the STFD wavefunctions is 2·04 and 2·10 for $n = 6$ and $n = 7$ respectively. The measurements by Penkin & Shabanova require normalization factors of 1·37 and 1·70. The present method indicates that Eberhagen's published oscillator strengths should be multipled by a factor of 0·483 to place them on an absolute scale.

4.2.2 *The Sr abundance.* The equivalent width for the resonance line ($\lambda_\odot$ = 4607·338 Å) was recently measured by Grevesse (1966) from high quality tracings obtained at the Jungfraujoch Station. These records which are superior with regard to resolution and signal-to-noise ratio permit a more accurate determination of the equivalent width than was achieved from earlier photoelectric and photographic recordings. Grevesse obtained W_λ = 50·3 mÅ which is to be compared with W_λ = 44 mÅ measured off the McMath–Hulbert tracings (Holweger 1967) and W_λ = 36 mÅ given in the RRT. Adopting W_λ = 50·3, the abundance [Sr] = +0·05 is obtained.

The revision in the absolute scale for the oscillator strengths of the excited lines of Sr I increased rather than decreased the abundance discrepancies noted by GMA between these lines and the resonance line. With the equivalent widths reported by GMA, the average abundance is [Sr] $\simeq$ +0·7, that is a factor of between 4 and 5 greater than is obtained from the resonance line. Inspection of the Utrecht Atlas indicates that the equivalent widths for these lines should be considered very uncertain. The apparent discrepancy is most probably attributable to gross errors in the W_λ measurements or to spurious identifications of Fraunhofer lines. It is most unlikely that the adopted oscillator strengths are in error by such a large factor. Remeasurement of the weak lines on high quality scans is necessary, with observations of the following lines, which are least blended, having first priority 7070·10, 6878·38, 5521·79, 5486·12, and 4741·92 Å. The observations should be made over a range in zenith distance in order to distinguish solar and terrestrial lines. A study of the centre–limb variation would also be valuable.

4.3 *The Sr II spectrum*

4.3.1 *Introduction.* The Sr II spectrum is represented in the solar spectrum by ten lines but six are unsuitable for an abundance analysis. The resonance lines $5s\ ^2S$–$5p\ ^2P^0$ at 4077 (W_λ = 405 mÅ) and 4215 Å (W_λ = 233 Å) are too strong to permit a satisfactory analysis. The cores of these lines are formed in regions ($\log \tau_0 \leq -4{\cdot}0$) of the solar atmosphere for which the information on temperatures and pressures is inadequate and in the outer layers non-LTE effects affecting the populations of the lowest levels may exist. The multiplet $5p\ ^2P^0$–$5d\ ^2D$ is especially unsuitable since each line is listed in the RRT as a blend of Sr II and another species. The four lines which are selected for the abundance analysis are listed in Table VII. A further line $5s\ ^2P_{3/2}{}^0$–$6s\ ^2S_{1/2}$ is seriously blended and is omitted.

TABLE VII

Sr II lines in the solar spectrum

RMT No.	Multiplet	ΔJ	$\lambda_\odot$ (Å)	χ (eV)	log gf*	W_λ (mÅ)	log $\frac{W_\lambda}{\lambda}+7$	[Sr]
2	$4d\,^2D$–$5p\,^2P^0$	$\frac{5}{2}$–$\frac{3}{2}$	10327·360	1·84	−0·24	165	2·20	+0·32
		$\frac{3}{2}$–$\frac{3}{2}$	10036·670	1·81	−1·19	72	1·86	
		$\frac{3}{2}$–$\frac{1}{2}$	10914·88	1·81	−0·48	152	2·14	+0·30
3	$5p\,^2P^0$–$6s\,^2S$	$\frac{1}{2}$–$\frac{1}{2}$	4161·799	2·94	−0·50	32	1·89	+0·27

* See Section 4.3.2.

The equivalent widths measured by de Jager & Neven (1967) are adopted. Grevesse (1966) measured the equivalent width for λ 4161 off Jungfraujoch tracings and this accurate determination is adopted.

4.3.2 *Oscillator strengths.* Lifetime measurements for the $5p\,^2P_{1/2,\,3/2}$ levels have been obtained using the Hanle effect and include direct measurements of the branching ratios (Gallagher 1967). The oscillator strengths obtained for the $4d\,^2D$–$5p\,^2P$ transitions are as follows:

$$^2D_{5/2}\text{–}^2P_{3/2} \quad gf = 0{\cdot}57 \pm 0{\cdot}12$$
$$^2D_{3/2}\text{–}^2P_{3/2} \quad 0{\cdot}064 \pm 0{\cdot}12$$
$$^2D_{3/2}\text{–}^2P_{1/2} \quad 0{\cdot}33 \pm 0{\cdot}06$$

The values computed from the STFD wavefunctions are 0·444, 0·487 and 0·230 respectively. The experimental oscillator strengths will be adopted but owing to the large uncertainty for $^2D_{3/2}$–$^2P_{3/2}$ this transition will not be included in the abundance analysis.

Experimental measurements are not available for the $5p$–$6s$ transition. However, the theoretical calculations are expected to be reliable and the tabulated result is taken from Warner (1968b).

4.3.3 *The Sr abundance.* The three Sr II lines considered in the abundance analysis give very similar results for the abundance. The mean value is [Sr] = +0·30. This result is significantly greater than the value [Sr] = +0·05 obtained from the Sr I resonance line. Since both results are based on accurate lifetime measurement of the oscillator strengths, it would appear unlikely that the discrepancy is attributable to systematic errors affecting one or both oscillator strength scales. It would appear that the result is probably the consequence of errors or deficiencies in the model atmosphere or in the adopted assumptions and procedure for calculating line profiles.

This conclusion is supported by a comparison of observed and computed line profiles for Sr II λ 10036 (Fig. 4). The observations are taken from de Jager & Neven (1967). The mismatch of the observed and computed profile is similar to the previously noted discrepancies for the Mg II profiles.

It might be argued that the discrepancies in Sr I and Sr II (also in Mg I and Mg II but not Ca I or Ca II) might be resolved by a modification of the adopted temperature (and pressure) distribution. However, it can be seen that such simple modifications will not resolve the profile discrepancies displayed for Mg II in Fig. 2 and for Sr II in Fig. 4. A more fundamental modification appears to be necessary.

In Section 2.2.3, it was suggested that it may be necessary to introduce an inhomogeneous model with a convective velocity field.

The discrepancy between the Sr I and Sr II results and the lack of a quantitative explanation limits the accuracy of the Sr abundance determination. Here, double weight is apportioned the Sr II result because three lines are available compared with one in Sr I. Then the mean abundance is [Sr] = +0·22, or

$$\log N(\mathrm{Sr}) = 2{\cdot}82.$$

The uncertainty in this result is difficult to estimate, but $\sim \pm 0{\cdot}2$ is probably a suitable compromise between the optimistic and pessimistic outlooks.

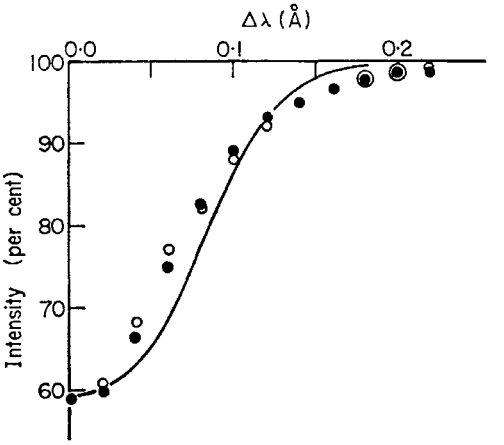

FIG. 4. *Line profiles for the Sr* II *line at* 10 036·66 *Å. The observed profile for the centre of the disk is taken from the observations of de Jager & Neven* (1967)*: see caption to Fig.* 2. *The predicted profile (solid line) has the same equivalent width as the observed profile.*

5. *Barium*

5.1 *Introduction.* Lines of the Ba I spectrum are absent from the photospheric spectrum. This discussion of the barium abundance is based on measurements of the Ba II lines in the photospheric spectrum. The accepted identifications for Ba II lines were extracted from the RRT and details are given in Table VIII. It is shown below that the suggested identification for the $6p$–$7s$ transition array must be considered questionable.

5.2 *Oscillator strengths.* Experimental measurements of the oscillator strengths are available for 5 of the 10 lines listed in Table VIII. These measurements are derived from lifetime determinations for the $6\,^2P_{1/2,\,3/2}{}^0$ levels using the Hanle effect (Gallagher 1967). Other experimental evidence is limited but consistent with the accurate lifetime results. Bucka, Eichler & von Oppen (1966) independently determined the lifetime of the $6p\,^2P_{3/2}{}^0$ level and obtained $(7{\cdot}0 \pm 0{\cdot}6) \times 10^{-9}$ s which is in agreement with Gallagher's measured value of $(6{\cdot}27 \pm 0{\cdot}25) \times 10^{-9}$ s. The hook method (Ostrovskii & Penkin 1961a, 1961b) has been used to measure the oscillator strength for the Ba II resonance lines (λ 4554, 4934) in terms of the resonance lines of the barium atom. Gallagher points out that with recent accurate lifetimes for Ba I a new normalization of the relative hook measurements can be undertaken. One obtains $gf(\lambda\,4554) = 1{\cdot}38$ with an uncertainty of about 20 per cent. The direct lifetime measurements give $gf(\lambda\,4554) = 1{\cdot}48 \pm 0{\cdot}10$.

Since the $5d$ level in Ba II is non-coulombic ($n^* \leq l+1$), the experimental results

TABLE VIII

Ba II *lines in the solar spectrum*

RMT No.	Multiplet	ΔJ	$\lambda_\odot$ (Å)	χ (eV)	log gf exp (G)	log gf Th (W)	W_λ (mÅ)	$\log \frac{W_\lambda}{\lambda}+7$	[Ba]*	Remarks†
1	$6s^2S$–$6p^2P^0$	$\frac{1}{2}$–$\frac{3}{2}$	4554·036	0·00	+0·17	+0·19	169	2·57	−0·04	159RRT, 180HOL, 162GMA, 173A
		$\frac{1}{2}$–$\frac{1}{2}$	4934·095		−0·15	−0·13	154	2·50	+0·12	117RRT, 160GMA, 184A
2	$5d^2D$–$6p^2P^0$	$\frac{5}{2}$–$\frac{3}{2}$	6141·727	0·70	−0·08	−0·16	121	2·29	−0·06	113RRT, 130GMA, 120A, (1)
		$\frac{3}{2}$–$\frac{3}{2}$	5853·688	0·60	−1·00	−1·16	58	2·00	−0·26	55RRT, 62HOL, 57GMA, 60A
		$\frac{3}{2}$–$\frac{1}{2}$	6496·908		−0·37	−0·46	98	2·18	−0·25	98RRT, 97HOL, 95GMA, 104A
3	$6p^2P^0$–$7s^2S$	$\frac{3}{2}$–$\frac{1}{2}$	4899·917	2·72		−0·08	57	2·07	+0·88	RRT (2), (3)
		$\frac{1}{2}$–$\frac{1}{2}$	4524·944	2·51		−0·54	31	1·84	+0·69	32RRT, 30GMA, 31A, (3)
4	$6p^2P^0$–$6d^2D$	$\frac{3}{2}$–$\frac{5}{2}$	4130·657	2·72		+0·56	37	1·95	−0·09	45RRT, 34GMA, 32A
		$\frac{3}{2}$–$\frac{3}{2}$	4165·999			−0·39	9	1·33	+0·07	RRT, (4)
		$\frac{1}{2}$–$\frac{3}{2}$	3891·781	2·51		+0·23	27	1·84	−0·13	30RRT, 25GMA

Notes:

* For RMT 1 and 2 results refer to experimental gf-values, and for RMT 3 and 4 to theoretical gf-values.

† HOL ≡ Holweger (1967).
A ≡ Allen (1934).

(1) In the RRT, this line is given as a blend of Ba II and Fe I.
(2) The RRT gives La II and Ti I as additional contributors.
(3) The results to [Ba] strongly suggest that Ba II may not be the principal contributor to this Fraunhofer line.
(4) The RRT lists a CN line as a contributor.

are adopted for the abundance analysis. For $6s\ ^2S$–$6p\ ^2P^0$, the results from lifetime measurements are in good agreement with the recent calculations by Warner (1968b) (see Table VIII). No experimental measurements are available for other multiplets and Table VIII lists only the calculated values.

5.3 *The Ba abundance.* The present discussion of the barium abundance is considered an interim report pending re-observation of several lines with the low-noise photoelectric spectrometers which are now in operation. The primary purpose of this discussion is to emphasize the necessity for new observations.

The equivalent widths for the resonance lines given by various observers are listed in the Remarks column of Table VIII. The weaker line λ 4934 is difficult to measure owing to the presence of a Fe I line of a similar intensity only 65 mÅ distant. The scatter in the independent estimates of the equivalent width reflects this blending. No weight should be assigned to the abundance derived from this line. More accurate observations and a thorough treatment of the blend are required before a reliable result can be obtained. The stronger line at 4554 Å is free from serious blending. The total range in the measured equivalent widths correspond to an abundance range $-0{\cdot}15 < [\mathrm{Ba}] < +0{\cdot}04$.

The multiplet RMT 2 probably provides the most favourable opportunity for an abundance determination. The leading line at 6141 Å is blended with an Fe I line and this is reflected in the larger abundance obtained from this line. The line is supposed unsuitable and is discarded. An inspection of the Utrecht Atlas shows that the other lines of the multiplet are not affected by blending; note that the individual measurements of W_λ are in good accord and, furthermore, the lines give almost identical results for the abundance.

The two lines from RMT 3 are ascribed solar identifications but give values for [Ba] which are not in accord with the results from other lines. It is unlikely that the theoretical oscillator strengths are in error by the necessary large factor. Therefore, it is suggested that Ba II is not the principal contributor to these Fraunhofer lines.

The lines from RMT 4 fall in a crowded region of the spectrum where accurate measurement of the equivalent width is difficult. The line λ 4165 is blended with a CN line and this is reflected in the result for [Ba].

In deriving the mean abundance, weight 4 is given to λλ 5853, 6496 from RMT 2, weight 2 to λ 4554, and weight 1 to λλ 4130, 3891. Experimental oscillator strengths are adopted for RMT 1 and 2. Theoretical oscillator strengths for RMT 4 are adopted in the absence of accurate experimental values. The following lines are rejected as unsuitable λλ 4934, 6141, 4899, 4524 and 4165. The mean abundance is $[\mathrm{Ba}] = -0{\cdot}20$. If theoretical oscillator strengths are adopted for all lines, the mean is increased to $[\mathrm{Ba}] = -0{\cdot}12$. The former value is preferred and the barium abundance is

$$\log N(\mathrm{Ba}) = 1{\cdot}90.$$

The reduction from the GMA value is attributable to two factors. Firstly, the damping constants have been included whereas GMA assumed the damping constant to be zero. Secondly, the adopted oscillator strengths—in particular for RMT 2—are less than the GMA values.

The desirability of improved observations is apparent from the above discussion. In particular, it is necessary to examine how the resonance line λ 4554 can be reconciled with the weaker lines from the $5d\ ^2D$–$6p\ ^2P^0$ multiplet. Finally, it might

be pointed out that line profile observations of the highest attainable accuracy might lead to a determination of the isotopic abundances. The isotopic shifts are small (0·006 to 0·010 cm^{-1} for the resonance lines (Arroe 1950)) but the hyperfine structure in the odd isotopes Ba^{137} and Ba^{139} (with natural abundances of 11·3 and 6·6 per cent respectively), which has a total width of about 0·25 cm^{-1} for the resonance lines, might be detectable in accurate observations of the line cores. The lines at 5853 and 6496 Å are probably more suitable but lack accurate laboratory measurement of the isotopic shifts and hyperfine structures. Similar comments on isotopic abundance determination are applicable to the other alkaline earths.

6. *Concluding remarks*

The abundances we have derived for the alkaline earths in the Sun are as follows:

	Neutral	Ionized	Recommended
Mg	7·36	7·59	7·48
Ca	6·33	6·33	6·33
Sr	2·65	2·90	2·82
Ba	—	1·90	1·90

We feel that the difficulty of calculating accurate oscillator strengths for the neutral spectra of the alkaline earths may be to some extent responsible for the discrepancy between Mg I and Mg II. Our successful treatment of Ca I results from the availability of an excellent series of experimental relative *f*-values and we would urge that a similar set of data for Mg I should be produced as soon as possible.

Improvements in the Sr and Ba abundances can only come from extensive measurements of the weaker lines of these elements; new determinations of equivalent widths and *f*-values are required. Our abundance values quoted above can be considered only as preliminary attempts to improve on the GMA discussion.

Acknowledgment. Part of this work was performed while one of us (B. W.) held the Radcliffe–Henry Skynner Senior Research Fellowship in Astronomy at Balliol College, Oxford.

D. L. Lambert:
Mount Wilson and Palomar Observatories,
Carnegie Institution of Washington,
California Institute of Technology,
Pasadena,
California.

B. Warner:
Department of Astronomy,
University of Texas,
Austin,
Texas.

1967 *December.*

References

Allen, C. W., 1934. *Mem. Commonw. Solar Obs., Mt. Stromlo,* No. 5.
Arroe, O. H., 1950. *Phys. Rev.,* **79,** 836.
Babcock, H. D. & Moore, C. E., 1947. *The Solar Spectrum* λ 6600–λ 13495, Carnegie Institute, Washington.
Bucka, H., Eichler, J. & Oppen, G. V., 1966. *Z. Naturf.,* **21a,** 654.
de Jager, C. & Neven, L., 1967. *Bull. astr. Insts Neth., Suppl. Ser.,* **1,** 325.
Delbouille, L. & Roland, G., 1963. *Photometric Atlas of the Solar Spectrum from* λ 7498 *to* λ 12016, Liège.

Dumont, S., 1967. *Ann. d'Astrophys.*, **30**, 421.
Eberhagen, A., 1955. *Z. Phys.*, **143**, 392.
Edlén, B. & Risberg, P., 1956. *Ark. Fys.*, **10**, 553.
Gallagher, A., 1967. *Phys. Rev.*, **157**, 24.
Goldberg, L., Müller, E. A. & Aller, L. H., 1960. *Astrophys. J., Suppl. Ser.*, **5**, 1.
Grevesse, N., 1966. *Ann. d'Astrophys.*, **29**, 287.
Holweger, H., 1967. *Z. Astrophys.*, **65**, 365.
Hulpke, E., Paul, E. & Paul, W., 1964. *Z. Phys.*, **177**, 257.
Lambert, D. L., 1968. *Mon. Not. R. astr. Soc.*, **138**, 143.
Lambert, D. L. & Warner, B., 1968a. *Mon. Not. R. astr. Soc.*, **138**, 181.
Lambert, D. L. & Warner, B., 1968b. *Mon. Not. R. astr. Soc.*, **138**, 213.
Lurio, A., de Zafra, R. L. & Goshen, R. J., 1964. *Phys. Rev.*, **134**, 1198.
Minnaert, M. G. J., Mulders, G. F. W. & Houtgast, J., 1940. *Photometric Atlas of the Solar Spectrum* 3332 *Å to* 8771 *Å*, Schnabel, Amsterdam.
Mitchell, W. E., 1959. *Astrophys. J.*, **129**, 93.
Mohler, O. C., 1955. *A Table of Solar Spectrum Wavelengths* 11 984–25 578 *Å*, University of Michigan Press, Ann Arbor.
Moore, C. E., Minnaert, M. G. J. & Houtgast, J., 1966. *The Solar Spectrum* 2395–8770 *Å*, National Bureau of Standards, Washington.
Müller, E. A. & Mutschlecner, J. P., 1964. *Astrophys. J., Suppl. Ser.*, **9**, 1.
Olsen, K. H., Routly, P. M. & King, R. B., 1959. *Astrophys. J.*, **130**, 688.
Ostrovskii, Yu. I. & Penkin, N. P., 1961a. *Opt. Spectrosc.*, **10**, 3.
Ostrovskii, Yu. I. & Penkin, N. P., 1961b. *Opt. Spectrosc.*, **11**, 307.
Penkin, N. P. & Shabanova, L. N., 1965. *Opt. Spectrosc.*, **18**, 535.
Prokofiev, V. K., 1928. *Z. Phys.*, **50**, 701.
Risberg, P., 1955. *Ark. Fys.*, **9**, 483.
Smith, W. W. & Gallagher, A., 1966. *Phys. Rev.*, **145**, 26.
Swensson, J. W. & Risberg, G., 1966. *Ark. Fys.*, **31**, 237.
Trefftz, E., 1951. *Z. Astrophys.*, **29**, 287.
Utrecht Observatory Staff, 1960. *Rech. astr. Obs. Utrecht*, **15**.
Warner, B., 1968a. *Mon. Not. R. astr. Soc.*, **139**, 1.
Warner, B., 1968b. *Mon. Not. R. astr. Soc.*, **139**, 115.
Warner, B., 1968c. *Mon. Not. R. astr. Soc.*, **139**, 103.